tween theory and experiment shows that the experimental data are well predicted by the present nonlinear theory for all rear positions of the wing, whereas the results of the linear theory show good agreement for very small angles of incidence only. The pitching moment curves $C_m(\alpha_\infty)$ are plotted in Fig. 2b for five different rear positions of the wing. The present nonlinear theory gives excellent agreement with the experimental data for all wing positions. The improvement achieved by the nonlinear theory compared with the linear theory is remarkable.

The results of sample calculations carried out on slender body mid-wing configurations for other body shapes and other wing plan forms show also fairly good agreement with experimental results.[4]

References

[1]Gersten, K., "Nichtlineare Tragflächentheorie, insbesondere für Tragflügel mit kleinem Seitenverhältnis," Habilitationsschrift Braunschweig 1960. *Ingenieur Archiv*, Vol. 30, 1961, pp. 431–452.

[2]Gersten, K., "A Nonlinear Lifting-Surface Theory Especially for Low-Aspect-Ratio Wings," *AIAA Journal*, Vol. 1, No. 4, April 1963, pp. 924–925.

[3]Hafer, X., "Untersuchungen zur Aerodynamik der Flügel-Rumpf-Anordnungen," Dissertation Braunschweig, 1957. Jahrbuch 1957 der Wissenschaftlichen Gesellschaft für Luftfahrt (WGL), 1958, pp. 191–207.

[4]Otto, H., "Ein Beitrag zu den nichtlinearen Auftriebs- und Nickmomenteneigenschaften von schlanken Flügel-Rumpf-Kombinationen," Dissertation Braunschweig, 1972. Bericht 72/7 des Institutes für Strömungsmechanik der Technischen Universität Braunschweig, 1972; also Deutsche Luft- und Raumfahrt (DLR), Forschungsbericht (FB) 73-66, 1973; and Zeitschrift für Flugwissenschaften (ZFW), Vol. 22, 1974, pp. 187–200.

Some Characteristics of Airfoil-Jet Interaction with Mach Number Nonuniformity

C. Edward Lan*

The University of Kansas, Lawrence, Kan.

Introduction

A STOL concept of current interest is the upper surface blowing configuration where the high-velocity jet from high-bypass-ratio engines blows over the wing surface. The high lift derives not only from the Coanda effect when the flap is deflected, but also from the aerodynamic interaction with the relatively thick jet. Shollenberger[1] has analyzed a similar configuration including the effects of 2-D nacelle and jet distortion. The case where the airfoil is in a midstream of one velocity with different velocity regions above and below has been treated by Ting and Liu.[2] In both investigations the flow has been assumed 2-D, inviscid, and incompressible. The effect of Mach number nonuniformity where the jet Mach number is different from the freestream value has not been investigated. The Mach number nonuniformity may occur not only at low speed with high thrust but also at high-speed cruise flight.

Received April 11, 1974; revision received May 6, 1974. This research is part of a project supported by NASA Grant 17-002-107.

Index category: Aircraft Aerodynamics (Including Component Aerodynamics).

*Associate Professor of Aerospace Engineering. Member AIAA.

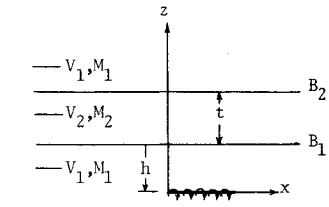

Fig. 1 Geometry definition.

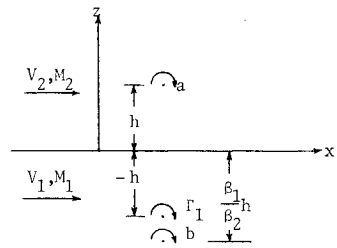

Fig. 2 Vortex images.

In this Note, the image method will be used to examine the upper-surface-blowing jet-airfoil interaction with Mach number nonuniformity. The formulation represents an extension of the classical incompressible results.[2,3] Some characteristics of the interaction will be discussed. The main assumptions are 1) inviscid linear theory, 2) two-dimensional jet, 3) no turbulent mixing, and 4) no airfoil thickness effect.

Mathematical Formulation

A plane jet with Mach number M_2 is assumed to be imbedded in a freestream of Mach number M_1. A thin airfoil is placed at a distance h below the lower jet surface, as shown in Fig. 1. For $h = 0$, this may represent an idealized configuration with upper-surface blowing jet. The induced velocity vector due to a two-dimensional vortex with strength Γ in the linearized compressible flow can be shown to be[4]

$$\mathbf{q} = (\Gamma\beta/2\pi)(\mathbf{i}(z - z') - \mathbf{k}(x - x'))/((x - x')^2 + \beta^2(z - z')^2) \quad (1)$$

where $\beta = (1 - M^2)^{1/2}$. To examine how disturbances reflect and diffract at the interface of two flows of different energy levels, consider a vortex of Γ_1 at $z' = -h$ in region 1 (See Fig. 2). The boundary conditions at $z = 0$ are[3]

$$w_1/V_1 = \dot{w}_2/V_2 \quad \text{(Flow tangency)} \quad (2)$$

$$\rho_1 V_1 u_1 = \rho_2 V_2 u_2 \quad \text{(Pressure continuity)} \quad (3)$$

Because of the presence of the vortex Γ_1 at $(x', -h)$, the flowfield in region 2 will be disturbed. Following Koning's concept[3] for incompressible flow, a vortex of strength b at $z' = -\beta_1 h/\beta_2$ will be introduced. It follows that the induced flow in region 2 can be written as

$$\mathbf{q}_2 = \frac{b\beta_2}{2\pi} \frac{\mathbf{i}(z + \beta_1 h/\beta_2) - \mathbf{k}(x - x')}{(x - x')^2 + \beta_2^2(z + \beta_1 h/\beta_2)^2} \quad (4)$$

On the other hand, the disturbance due to the vortex Γ_1 will be reflected back to region 1 at the interface, as represented by a vortex of strength "a" at the image point in region 2. Hence, the total induced flow in region 1 is

$$\mathbf{q}_1 = \frac{\Gamma_1\beta_1}{2\pi} \frac{\mathbf{i}(z + h) - \mathbf{k}(x - x')}{(x - x')^2 + \beta_1^2(z + h)^2} + \frac{a\beta_1}{2\pi} \frac{\mathbf{i}(z - h) - \mathbf{k}(x - x')}{(x - x')^2 + \beta_1^2(z - h)^2} \quad (5)$$

Using Eqs. (4) and (5) together with Eqs. (2) and (3), the unknown vortex strengths a and b can be found to be

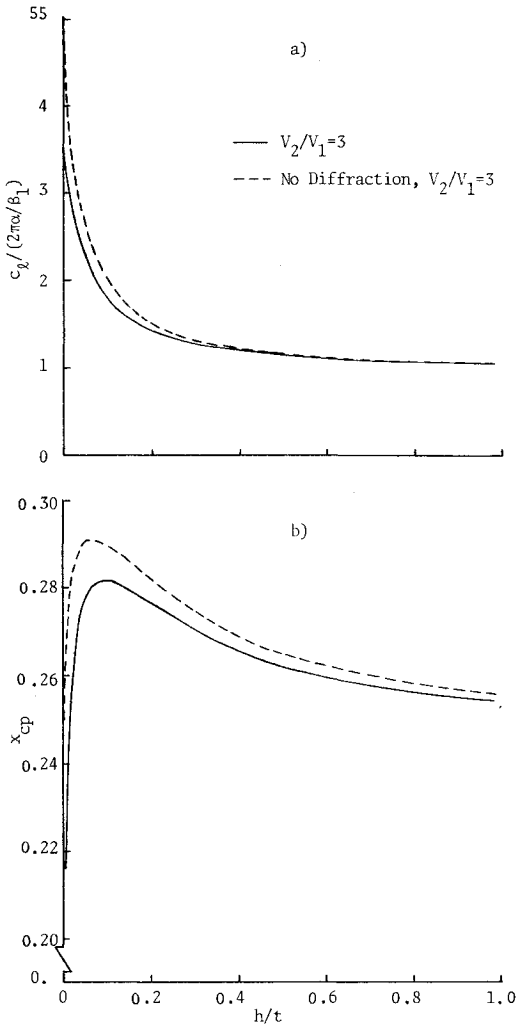

Fig. 3 Aerodynamic characteristics of a flat-plate airfoil with jet interaction in incompressible flow. t/c = 0.5.

$$a = -\Gamma_1\left(\frac{\rho_2 V_2^2}{\rho_1 V_1^2} - \frac{\beta_2}{\beta_1}\right)\Big/\left(\frac{\rho_2 V_2^2}{\rho_1 V_1^2} + \frac{\beta_2}{\beta_1}\right) = \lambda_{12}\Gamma_1 \quad (6)$$

$$b = \Gamma_1\left(2\frac{V_2}{V_1}\right)\Big/\left(\frac{\rho_2 V_2^2}{\rho_1 V_1^2} + \frac{\beta_2}{\beta_1}\right) = \delta_{12}\Gamma_1 \quad (7)$$

Equations (6) and (7) show that the parameters determining the additional vortex strength "a" of the reflected disturbances and the vortex strength "b" for the diffracted disturbances are the dynamic pressure ratio, the velocity ratio and the β ratio. In incompressible flow, Eqs. (6) and (7) agree with those given by Koning.[3]

Now apply the above results to the configuration shown in Fig. 1. Define z_1 and z_2 as the distances from the lower and upper jet boundaries, B_1 and B_2, respectively. The distance will be regarded as positive if the vortex is above the boundary. The reflection of disturbances from region 2 into region 1 is characterized by the reflection coefficient λ_{12} which is equal to a/Γ_1 of Eq. (6) and the diffraction from region 1 into region 2 by δ_{12} which is equal to b/Γ_1 of Eq. (7). Similar definitions can also be applied to define λ_{21} and δ_{21} by interchanging the subscripts 1 and 2 in Eqs. (6) and (7). Now a vortex γ at a distance h from B_1 (or $z_1 = -h$) is reflected at B_1, with an additional vortex $\lambda_{12}\gamma$ at $z_1 = +h$ and diffracted into the midstream with a vortex $\delta_{12}\gamma$ at $z_1 = -\beta_1 h/\beta_2$. The diffracted disturbance is then reflected at B_2 to give an additional vortex $\delta_{12}\lambda_{21}\gamma$ at $z_2 = \beta_1 h/\beta_2 + t$. The reflected disturbances are in turn reflected and diffracted at B_1. The diffracted disturbances into the lower region are due to the vortex $\delta_{12}\lambda_{21}\delta_{21}\gamma$ at $z_1 = (\beta_1 h/\beta_2 + 2t)\ \beta_2/\beta_1 = h + 2t\beta_2/\beta_1$, and so on. Adding the

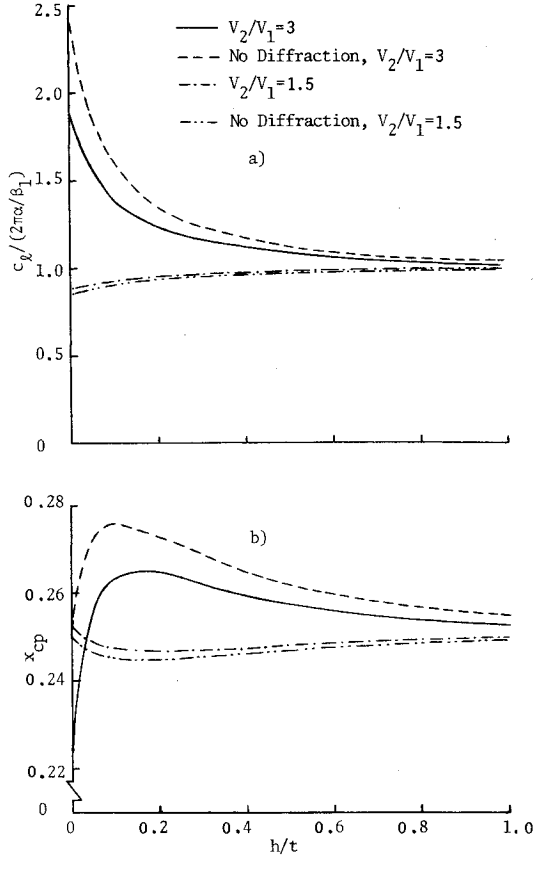

Fig. 4 Aerodynamic characteristics of a flat-plate airfoil with jet interaction in linearized compressible flow. t/c = 0.5, M_1 = 0.4, and T_2/T_1 = 3.

effects of all image vortices in the upper stream gives the total diffracted disturbances in the lower stream. With reference to the airfoil coordinate system, the downwash produced at the airfoil is given by

$$w(x,0) = -\frac{\beta_1}{2\pi}\int_0^1 \left\{\frac{1}{x-x'} + \frac{\lambda_{12}(x-x')}{(x-x')^2 + \beta_1^2 4h^2} + \delta_{12}\delta_{21}\lambda_{21}\sum_{i=1}^{\infty}\frac{\lambda_{21}^{2i-2}(x-x')}{(x-x')^2 + 4\beta_1^2(h + it\beta_2/\beta_1)^2}\right\}\gamma(x')dx' \quad (8)$$

where the downwash is normalized with respect to V_1 and all lengths are based on the chord length. The second term inside the integral of Eq. (8) will be called the reflection term and the last the diffraction terms. The boundary condition is

$$w(x,0) = dzc/dx - \alpha. \quad (9)$$

To solve Eqs. (8) and (9), the classical airfoil method of Ref. 2 is used and its computer program revised for the presssent purpose.[4]

Numerical Results and Discussions

For completeness and for comparison purposes, one set of incompressible results is presented in Fig. 3 for t/c = 0.5. For the linearized compressible flow, T_2/T_1 = 3 and M_1 = 0.4 were assumed. The Mach number ratio and the density ratio are computed as $(M_2/M_1)^2 = (V_2/V_1)^2(T_1/T_2)$ and $\rho_2/\rho_1 = T_1/T_2$. The results are shown in Fig. 4. Figure 5 shows how the Mach number nonuniformity affects the aerodynamic characteristics. From the numerical results presented, the following observations can be made. Note that the "no diffraction" curves are the case where all diffraction terms in Eq. (8) are ignored.

1) From Figs. 3a and 4a, it is seen that the reflection coefficient λ_{12} is the primary parameter which determines

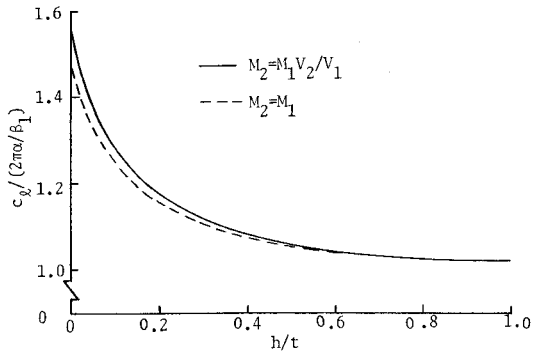

Fig. 5 Effect of Mach number nonuniformity on lift augmentation of a flat-plate airfoil. t/c = 0.5, M_1 = 0.4, T_2/T_1 = 1.0, and V_2/V_1 = 1.5.

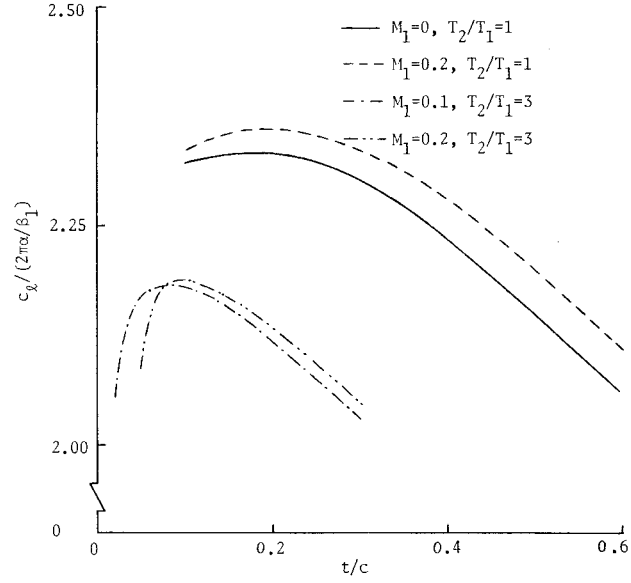

Fig. 6 Variation of lift augmentation with jet thickness, M_1 and T_2/T_1 at c_T = 2.095 for the upper surface blowing configuration.

the aerodynamic characteristics in the airfoil-jet interaction in either compressible or incompressible flow. A negative value of λ_{12} increases c_l. For example, in Fig. 4 for T_2/T_1 = 3 and M_1 = 0.4, λ_{12} = −0.5845 for V_2/V_1 = 3 and λ_{12} = 0.1542 for V_2/V_1 = 1.5. A positive λ_{12} yields lower lift. Therefore, for a given jet thickness ratio t/c, it may be possible to use λ_{12} to correlate the experimental data with jet interaction.

2) With positive lift augmentation as represented by $c_l/(2\pi\alpha/\beta_1) > 1$, Figs. 3b and 4b show that the aerodynamic interaction tends to shift the c.p. backward until the airfoil is close to the jet surface. It may also be concluded that diffracted disturbances tend to move the c.p. forward and reflected disturbances would move the c.p. in the opposite direction. Since the diffraction terms are important as the airfoil gets closer to the jet boundary, this explains why the c.p. will shift rapidly forward as the airfoil is moved toward the jet boundary. Since for a flat airfoil the locations of c.p. and a.c. coincide, it is seen that for the airfoil at the jet lower surface as in the upper surface blowing configuration, the a.c. will be shifted forward of $c/4$ point because of the interaction, a conclusion consistent with experimental results for a wing-body half model.[5] The shift is greater in incompressible flow than in compressible flow as seen from Figs. 3b and 4b.

3) For a given t/c, the higher the jet dynamic pressure relative to the freestream value, the faster the decrease in lift augmentation as h/t is increased. This means that raising the jet slightly above the airfoil surface would greatly decrease the lift augmentation for a high dynamic pressure jet.

4) Figure 5 shows that the lift is slightly increased for the higher jet Mach number with other parameters remaining unchanged. This fact can be explained by the more negative reflection coefficient. For T_2/T_1 = 1.0, V_2/V_1 = 1.5, and $M_1 = M_2$ = 0.4, λ_{12} can be computed to be −0.3846. On the other hand, if $M_2 = M_1(V_2/V_1)$ = 0.6, then λ_{12} = −0.4410. More negative reflection coefficient implies more lift. The lift increment is slight because the diffraction terms which are to decrease the lift are also increased. Since λ_{12} remains to be −0.3846 even if $M_1 = M_2$ = 0, the above results indicate that the lift augmentation, expressed as $c_l/(2\pi\alpha/\beta_1)$, in compressible flow with higher M_2 is higher than that in incompressible flow.

5) Comparing Figs. 4 and 5 for V_2/V_1 = 1.5, it may be concluded that high jet temperature has detrimental effects on lift as it would reduce the dynamic pressure. At T_2/T_1 = 3.0 and V_2/V_1 = 1.5, c_l is less than the uniform flow value because λ_{12} is now positive. Examining Figs. 3 and 4 for V_2/V_1 = 3.0, it is also seen that the lift augmentation for T_2/T_1 = 3.0 and M_1 = 0.4 is much less than that in the incompressible flow when the airfoil is close to the jet boundary. Therefore, wind-tunnel tests of wing-jet interaction with cold jet may overestimate the lift unless all flow parameters, in particular λ_{12}, are correctly simulated.

6) Consider the following observations for h = 0. a) With negative λ_{12}, i.e., the lift is increased over the uniform flow value, diffraction terms in Eq. (8) are to decrease the lift. These diffraction terms become unimportant as the jet thickness is increased. b) The lift is always increased when V_2/V_1 is increased.

Keeping these two facts (6a and b) in mind, now consider the case with a given amount of thrust. As the jet thickness is increased, the diffraction becomes less important so that the lift is increased, while the decrease in velocity ratio because of thicker jet is to decrease the lift. On the other hand, as the jet thickness is decreased, the above two effects reverse the trend. In the limit as $t \to 0$, the diffraction terms are so important that they exactly cancel the reflection effect so that the uniform-flow results are obtained. This can be shown by summing the coefficients inside the brackets in Eq. (8). This gives $f = 1 + \lambda_{12} + \delta_{12}\delta_{21}\lambda_{21}(1 + \lambda_{21}^2 + \lambda_{21}^4 + \ldots) = 1 + \lambda_{12} + \delta_{12}\delta_{21}\lambda_{21}/(1 - \lambda_{21}^2)$. However, for any β_1 and β_2, it can be easily shown that $\lambda_{21} = -\lambda_{12}$ and $\delta_{12}\delta_{21} = 1 - \lambda_{21}^2$. It follows that $f = 1 + \lambda_{12} + \lambda_{21} = 1$ independent of the velocity ratio. Therefore, as the jet thickness is increased from zero, the lift will be increased. Eventually, the lift will be decreased after reaching a maximum value because of the low velocity ratio associated with the large jet thickness. An optimum jet thickness is seen to exist. For the purpose of numerically computing the optimum jet thickness, a thrust coefficient c_T of 2.095 per unit span is assumed, a value taken directly from Ref. 5. This thrust coefficient will be defined as the amount of thrust divided by the jet thickness and the freestream dynamic pressure. By the momentum theory, the velocity ratio then depends on the jet thickness in accordance with the relation:

$$\frac{V_2}{V_1} = \frac{1}{2}\left[1 + \left(1 + \frac{2C_T}{(\rho_2/\rho_1)(t/c)}\right)^{1/2}\right] \qquad (10)$$

The results of computation are presented in Fig. 6. It is seen that an optimum jet thickness does exist. For T_2/T_1 = 1.0, the optimum thickness ratio t/c lies between 0.175 and 0.2, approximately independent of the Mach number. On the other hand, for T_2/T_1 = 3.0, the optimum t/c becomes 0.1.

References

[1]Shollenberger, C. A., "Analysis of the Interaction of Jets and Airfoils in Two Dimensions," *Journal of Aircraft*, Vol. 10, No. 5, May 1973, pp. 267–273.

[2]Ting, L. and Liu, C. H., "Thin Airfoil in Nonuniform Parallel Streams," *Journal of Aircraft*, Vol. 6, No. 2, March–April 1969, pp. 173–175.

[3]Koning, C., "Influence of the Propeller on Other Parts of the Airplane Structure," *Aerodynamic Theory*, Vol. IV, edited by W. F. Durand, Dover, New York, 1963, p. 361.

[4]Lan, C. E., "Compressibility Effects on Airfoil-Jet Interaction," Appendix B in "An Analytical Investigation of Wing-Jet Interaction," CRINC-FRL Rept. 74-001, April 1974, University of Kansas Center for Research, Inc., Lawrence, Kans.

[5]Phelps, A. E., Letko, W., and Henderson, R. L., "Low-Speed Wind-Tunnel Investigation of a Semispan STOL Jet Transport Wing-Body with an Upper-Surface Blown Jet Flap," TN D-7183, May 1973, NASA.

Evaluation of Drag Integral Using Cubic Splines

R. M. James*
Douglas Aircraft Company, Long Beach, Calif.
and
V. D. Panico†
Northwestern University, Evanston, Ill.

Introduction

THE well-known wave drag integral[1] which expresses the drag of suitably slender configurations in terms of an area distribution $S(x)$ can be written

$$I = -\frac{1}{2\pi}\int_0^1\int_0^1 S''(x)S''(y)\ \ln\ |x-y|\,dxdy \qquad (1)$$

This integral has been studied extensively in the past, notably by Eminton[2] to whom goes credit for the most widely used practical method of evaluation, given only a discrete point data set of values of $S(x_i)$. For most engineering applications, the input data set is quite crude whether the values represent areas or some other physical quantity arising from different calculations to which I applies. Nevertheless, $S(x)$ must be assumed to satisfy certain conditions, and the minimum necessary for Eq. (1) to be useful are:

$$\begin{aligned} &S'(x) \ \text{ is continuous in } \ (0 \le x \le 1) \\ &S'(0) = S'(1) = 0 \end{aligned} \qquad (2)$$

For the evaluation of drag when these conditions are not satisfied (in particular when $S'(x)$ is not continuous) more involved formulas than Eq. (1) alone are required,[3] but the restrictions, Eq. (2), are commonly assumed in practice and are required by Eminton's method.

Spline Techniques

With regard to the use of cubic (or other) splines in practical engineering, it is the authors' experience that all too often the initial enthusiasm is rapidly damped by the necessity for providing end conditions beyond mere point values in order to solve the usual tridiagonal matrix for the point second derivatives. If these extra conditions are not known with the same degree of precision as the point values of the function itself, then the spline formulation is no better than other simpler means of ad hoc interpolation. Many engineering applications start with poor quality input information, and under these circumstances splines are just another tool, not a panacea.

However, the conditions (2) are ready made for a spline assumption since the end derivatives are given exactly. Therefore, it was decided to test the accuracy of a spline method of evaluation of I by fitting the area distribution with a cubic spline using a standard subroutine for rapid solution of the usual tridiagonal matrix—essentially by Gaussian elimination. Such a method, it was felt, might be quicker than Eminton's and would not require the inversion of a full matrix and so might not be subject to the usual problems arising from large full matrix operations (e.g., large computer core requirements).

This idea, obvious as it is, had not attracted much attention until recently. Halfway through the runs described in this Note, the work of V. V. Shanbhag[4] came to the authors' attention; but it was decided to publish these results anyway as a further source of comparison cases.

It should be noted that the Eminton method has a design aspect in the sense that the eventual interpolation provides a body of minimum drag subject to the given constraint of having specified areas at certain x stations. Such a facility cannot necessarily be claimed for the spline method, but the purpose of this Note is merely to compare some evaluations. A more comprehensive view of these methods must be left to the practicing designers in this field.

Calculation Procedure

If $S(x)$ is given as a polynomial in x subject to conditions (2), then it is easy to evaluate I analytically in terms of the numbers

$$I_{r,s} = -\frac{1}{2\pi}\int_0^1\int_0^1 x^r y^s\ \ln\ |x-y|\,dxdy$$

These have been computed at Douglas Aircraft Co. using the IBM 370/165 system and stored and tabulated (for quick hand estimates). By using these numbers an exact solution is readily available to provide a standard for comparison between the Eminton and spline methods. The Eminton calculations were obtained from a standard production subroutine using point values of $S(x)$ as input. For the spline calculations $S''(x)$ is piecewise linear and so with some tedious but minor manipulations I can be expressed in various condensed forms. It appears that the neatest involves fourth differences of $S_j = S(x_j)$, but from a computational accuracy point of view, the formula actually used had more of an "influence function" character, viz.:

$$I = \frac{3a_m a_1}{4\pi} - \frac{a_m}{\pi}\sum_{j=1}^{m-1} b_j[W_{j,m}] - \frac{a_1}{\pi}\sum_{j=1}^{m-1} b_j[W_{j,1}] - \frac{1}{2\pi}\sum_{k=1}^{m-1}\sum_{j=1}^{m-1} b_k b_j\langle Z_{j,k}\rangle$$

Received March 28, 1974; revision received May 14, 1974. This work was supported by the McDonnell Douglas Independent Research and Development Program.

Index categories: Aircraft Aerodynamics (Including Component Aerodynamics); Subsonic and Transonic Flow.

*Principal Engineer/Scientist, Aerodynamics Research Group.

†Currently Graduate Assistant, Dept. of Applied Mathematics, Northwestern University.